WESTFÄLISCHE
WILHELMS-UNIVERSITÄT
MÜNSTER

# Barcode Detection and Recognition in Non-constrained Systems

**Ausarbeitung**

Veranstaltung:
**Begleitendes Praktikum zu Computer Vision WS 2016/17**

| | |
|---|---|
| Themensteller: | **Prof. Dr. Xiaoyi Jiang** |
| | Dimitri Berh |
| | Andreas Nienkötter |
| Betreuer: | Aaron Scherzinger |
| Verfasser: | **Aleksej Matis** |
| | **Alexander Schlüter** |
| | **Kjeld Schmidt** |

# Barcode Detection and Recognition in Non-constrained Systems

Aleksej Matis, Alexander Schlüter, Kjeld Schmidt

24 March 2017

# Contents

# 1  Introduction

The goal of this project is to read barcodes in given images. The barcodes can be arbitrarily translated, rotated and scaled in the image. The perspective might be skewed and parts of the image might be out of focus or suffer from bad lighting and glare spots. These images are typically obtained by mobile phone cameras, without requiring the user to center the barcode in the image, or to wait until the autofocus is fully adjusted.

There are no time or performance constrains placed on our detection.

Let us first describe the structure of an EAN-13 barcode [5]: The smallest width of a bar is called the base width. A typical digit is encoded in four bars, alternating black and white, where the number of base widths of each bar is variable, but the total number of base widths of all four bars is seven. The exact number of base widths of each bar encodes a specific digit as well as a digit type, one of A, B or C.

A barcode is now composed as follows:

1. A left quiet zone,

2. a guard pattern, consisting of three bars, each one base width,

3. six digits of type A or B,

4. a center guard pattern, consisting of five bars, each one base width,

5. six digits of type C,

6. a guard pattern, same as 2.,

7. a right quiet zone.

The total number of base widths in a barcode is thus $3 + 6 \cdot 7 + 5 + 6 \cdot 7 + 3 = 95$. The pattern types (A or B) of the first six read digits encode the actual first digit of the barcode. The last digit is a check digit and has to match the digit obtained through a calculation based on the other digits.

We implemented and compared multiple methods, which can be divided into three general steps:

1. **Localization**: finding the general location and orientation of the barcode in the image

2. **Boundary Detection**: determining the barcode's left and right boundaries

3. **Reading**

# 2   Localization

In order to read a barcode, we first have to localize it in a given image. We implemented two approaches. Gradient+Blur is a simple algorithm, with which we had some initial success. We later discarded it in favor of the much more successful Line Segment Detector approach. Both are detailed in this chapter.

## 2.1   Gradient+Blur

Our initial localization attempt showed limited success, but is conceptually very simple. The Gradient+Blur approach seeks to exploit the strong boundaries between the (white) background area and black bars in a standard barcode. In a few words; Detect edges on the image, then blur the result to remove noise and apply a threshold to the result. Open and close the resulting shapes, then select the biggest one. We will now go trough the steps in more detail.

1. Edge Detection

   We begin by detecting edges with the Sobel operator. We calculate the absolute difference of the x- and y-gradients $|\partial_x I - \partial_y I|$, discarding direction information. This leads to slightly worse results for barcodes rotated by about 45 degrees. The resulting image will usually contain large amounts of noise. This is fixed in the next step.

2. Blur+Threshold

   Next, we blur the previous result to smooth out the noise and apply a threshold afterwards. The blur is a normalized box filter of size 9. Note that 'noise' here refers not only to image imperfections, but also noise in the absolute gradient which might be a result of complex textures or other sources. The threshold is not set as a constant brightness of 127. Instead, we calculate the mean brightness of the image, add that value to 255 and divide by 2. This simple extra step gives slightly better results when dealing with very noisy images.

3. Close Forms

   The next two steps are very similar operations. First we *close* the remaining white areas. This means we first dilate the image, then erode it by the same amount. Dilation creates a new image in which a pixel is set to white if there is

at least one white pixel within a given radius white in the original image. More intuitively, white pixels grow outwards. Erosion is the opposite operation; A pixel is set to black, unless all pixels in the radius are white. This *closes* empty spaces between neighboring and inside of structures, while structures with no neighbors will remain unchanged. At this point, the barcode will ideally have merged into a solid shape,

4. Open Forms

   Opening the forms is similar to closing, but in reverse order; First eroding, then dilating by the same amount. This will eliminate small structures (which is not actually important at this point), while straightening edges on larger structures.

5. Selection

   Finally, we select the largest structure to be the most likely location of the barcode in the original image. In most cases, our result will be a jagged shape, only roughly tracing a rectangle. To simplify matters going forward, we now find the minimal area rectangle around the selected structure. This will get passed into the boundary detection step.

## 2.2   LSD

This localization method is based on the LineSegmentDetector algorithm [4], which is implemented in OpenCV 3 in the cv::LineSegmentDetector class [1]. The algorithm detects line segments in an image, such as the segments formed by the bars in a barcode. On a high level, it works by first calculating the image gradient and assigning to each pixel a unit vector perpendicular to the gradient, resulting in a *level line field*. Pixels with a gradient magnitude under a certain tolerance are discarded. Connected pixels with similar level line angles are clustered together and form a *line support region*. To each line support region, a rectangle is fit which covers the whole region. To limit the number of false detections, the rectangle is only accepted as a line segment if the number of covered pixels with aligned level lines is high enough relative to the total number of covered pixels. The exact threshold is based on a statistical model (*a contrario* method), so that the rectangle is only accepted if, in a purely random level line field, the found ratio of aligned level lines is unlikely. Before a rectangle is rejected, some variations of the rectangle's parameters are tried.

The barcode localization method is taken from Creusot et al. [2] with minor modifications. First we run the LineSegmentDetector provided by OpenCV on the image. We use default parameters, except for the first parameter LSD_REFINE_NONE, which disables refinement of line segments. We found that line refinement tends to break up barcode bars into multiple segments, e.g. if the bars in the image are not quite straight due to kinks in the material on which the barcode is printed, or if there are glare spots on the barcode. This is undesirable, since in the following steps we rely on the length of line segments in the barcode to be similar.

Next we want to find a line segment which belongs to a barcode bar approximately in the middle of the barcode. To each detected line segment, a score is assigned based on how many other line segments might belong to bars of the same barcode as the first one. Two line segments are regarded as possibly belonging to the same barcode, if

1. their centers are not too far apart,

2. they have similar length,

3. they have similar angles and

4. their projected intersection covers most of the smaller segment.

Calculation of the first three distance measures is straightforward: Let $c_i$ be the center positions, $l_i$ the segment lengths and $\alpha_i$ the segment angles, where the index $i = 1, 2$ denotes the first or the second line segment, respectively. The used criteria are

$$d_{\text{center}} := \frac{\|c_1 - c_2\|}{l_1} < 1, \qquad \frac{|l_1 - l_2|}{l_1} < 0.3, \qquad |\alpha_1 - \alpha_2| < 0.1 \,.$$

Two lines fulfilling the first three criteria might still not be arranged like barcode bars, if they are displaced along the line direction. To catch these cases, we project the second line onto the first and check that the intersection is large enough relative to the length of the smaller line.

For each line segment which fulfills the criteria, Creusot et al. increment the score of the first line segment by one. Instead, we increment the score of the first line segment by $1 - d_{\text{center}}$. This effectively weighs the score by the distance between the line segments, which favors line segments which lie in the middle of the barcode.

Finally, we select the line segment with the highest score. This line segment should correspond to a barcode bar in the middle of the barcode.

# 3 Boundary Detection

To complement the LSD localizer, which returns a line segment in the middle of the barcode (hereafter called *best line*), we need to find the barcode's boundaries before we can attempt to read it.

## 3.1 Variation

The variation boundary finder is the original boundary detection method proposed in [2] in conjunction with the LSD localization. Let $L_\perp$ denote the sequence of intensity values along the line perpendicular to the best line, going through the best line's center (hereafter called *bisector*). Since barcodes consist of alternating black and white bars, the variation of intensity values along a line crossing the barcode is expected to be high. The boundary points are thus expected to have the following property: Extend a "probing" line (*inner probe*) from the boundary point along the bisector, pointing inside the barcode, i.e. in direction of best line's center. Extend a second "probing" line (*outer probe*) from the boundary point in the opposite direction, away from the barcode. The variation along the inner probe is now expected to be much higher than the variation along the outer probe.

To find the boundary points, for each index $k$ along the bisector, the signed variation difference

$$\phi_{L_\perp}(k) = \sum_{j=-R}^{0} |L_\perp(k+j) - L_\perp(k+j-1)| - \sum_{j=0}^{R} |L_\perp(k+j) - L_\perp(k+j+1)|$$

is computed. Here, $R$ is the probing distance, which we chose as $R = l_*/2$, half of the length of the best line.

The right boundary point should lie at the bisector index with maximal $\phi_{L_\perp}$, while the left boundary point should have minimal $\phi_{L_\perp}$.

We deviate slightly from Creusot et al. by instead using the variation measure

$$\phi_{L_\perp}^*(k) = \sum_{j=-R}^{0} |L_\perp(k+j) - L_\perp(k+j-1)| \cdot (R+j) - \sum_{j=0}^{R} |L_\perp(k+j) - L_\perp(k+j+1)| \cdot (R-j),$$

giving higher weight to pixel values near the current boundary candidate at index $k$.

## 3.2 LSD Bound

Motivated by the high quality of line segments returned by LineSegmentDetector, we constructed a new boundary finder, using ideas from the variation method described above. The goal is to determine the line segments corresponding to the two outer barcode bars, the *boundary segments*.

We first filter the line segments, so that only segments parallel to and located next to the best line are kept. To that end, we use the angle criterion and the criterion of sufficient projected intersection as described in section 2.2. Let $\{s_k\}_{k=1}^N$ be the sequence of remaining line segments and let $l_k$ be the length of the $k$-th segment. Let $\{c_k\}_{k=1}^N$ be the real numbers which result from the projection of the segment centers onto the bisector. We sort the segments by their center projection, such that $c_i < c_j$ for all $i < j$.

The boundary segments should have the following property: As before, extend an inner probe from the projected center of the boundary segment along the bisector, pointing inside the barcode. Extend an outer probe in the opposite direction, away from the barcode. The inner probe is expected to cross a large number of line segments which have not been filtered out in the previous step, while the outer probe is expected to cross very few such lines.

We used probing lines with length equal to the length of the best line, $l_*$. For each boundary segment candidate $s_k$, a score is assigned to both probes. For each other line segment $s_j$ that is crossed by the probe, the value

$$d_{jk} = (l_* - |c_j - c_k|) \cdot \max(0, l_* - |l_* - l_j|)$$

is added to the probing line's score. The first factor weighs line segments higher if they are close to the current boundary segment candidate. The second factor weighs segments higher if their length is close to the best line's length. To calculate the score of $s_k$, we now subtract the outer probe's score from the inner probe's score. On each side of the best line, we select the three segments with the highest score as final boundary candidates and try all combinations of those in the reading step.

## 3.3 Wachenfeld

Another implementation was adapted from the barcode detection and recognition algorithms proposed by Wachenfeld et al. [6]. The method is subdivided into the three steps of preprocessing, barcode edge detection and hypothesis based reading. Since

we implemented barcode localization (section 2) and barcode reading (section 4) as separate steps only the edge detection with a bit of preprocessing is adapted.

The originally proposed boundary detection assumes that the position of the barcode is centered. This way, a simple scan line can be applied to the picture. If the barcode is unreadable or misaligned the scan line can be reapplied with a rotation or shift factor. Since the position and rotation of the barcode is already determined in the localization step it is sufficient to place a scan line perpendicular to the best line. To simplify further steps we applying an affine transformation to the region around the scan line.

For the preprocessing we need to first detect to local maxima and minima. Our pictures are already converted to gray scale on loading so we can directly traverse the scan line from the middle pixel toward the outside and look for neighboring pixels with difference in value greater then a set threshold. In a second step we need to remove overly extreme points by executing a pruning step. Lastly we need to apply a dynamic threshold by always comparing every local extremum to an inwards neighborhood.

The boundary detection is based on some properties of the barcode. As shown in section 1, an EAN13 barcode consists of 59 black or white bars: $2 \times 3$ for the outer guards, 5 for the inner guard and $12 \times 4$ for the 12 digits.

To detect the boundaries we start with the middle pixel. If this pixel is white we look for the nearest black pixel. The corresponding black segment of this pixel is selected. From this selection we traverse toward the outsides by looking for the smallest neighboring pair of white and black segments to the left and right and adding it to the current selection. The selected region must at all times be enclosed by black segments. This process is demonstrated in fig. 1. The smallest pair of segments is required to prevent the algorithm from selecting structures beyond the quiet zone.

The outer guard bars are detected as soon as we have selected all 59 black and white segments respectively 29 pairs and the initial middle segment.
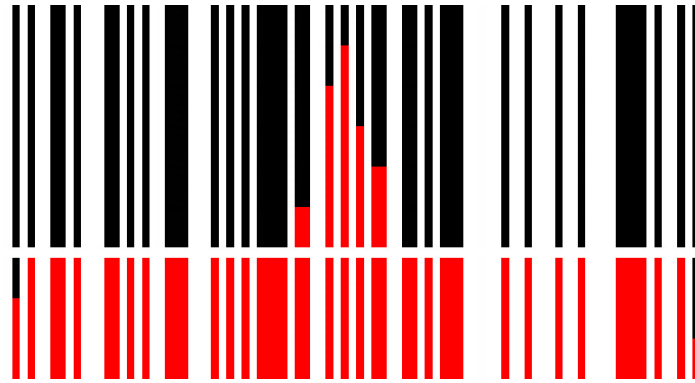
Figure 1: Application of the Wachenfeld boundary detection. The selection is colored in red. Steps are shown from top to bottom.

# 4 Reading

Our reading method is taken from [3] and is based on matching deformable templates to a 1D scanline obtained from the localization and boundary detection steps. From the previous steps, we get left and right boundary candidates as positions on the image, as well as the best line from the LSD step, the height of which we assume to be the height of the barcode. Since there are no time restrictions, we now try all combinations of left and right boundary candidates. For each left/right pair, we also try seven offsets along the height of the barcode and for each offset, we try both possible orientations (up/down). For example, if we get three left and three right boundary candidates from the LSD Bound step, a total number of $3 \cdot 3 \cdot 7 \cdot 2 = 126$ different scanlines would be tried.

Let $p_l$ and $p_r$ denote the positions of the current left and right boundary candidates. Since an EAN-13 barcode consists of 95 base widths, an initial estimate of the base width is $w = \|p_l - p_r\|/95$. Since the number of base widths in each pattern (guard or digit) is known, we can calculate an initial estimate of the offset along the scanline at which each pattern should begin. A naive (non-deformable) template matching algorithm would now match a template for each possible pattern (digits 0-9, types A,B and C) against the scanline, scaled such that the base width is $w$, starting at the estimated offset.

However, there is an uncertainty associated with the estimates, $\triangle w$ for the base width and $\triangle o$ for the offsets. These uncertainties are due to inaccuracies of the boundary detection, kinks in the material, etc. For example, if the perspective is skewed, the base width at the end of the barcode which is closer to the camera might be larger

than the base width at the farther end. In our implementation we chose $\Delta o = 3w$ and $\Delta w = 2\Delta o/95$. Based on a distance measure between templates and grey values on the scanline (for details see [3]), we calculate the matching probability for each possible template at each position. We integrate over every offset and base width in the ranges $[o - \Delta o, o + \Delta o]$ and $[w - \Delta w, w + \Delta w]$, scaling and translating the templates appropriately along the scanline. In addition to the matching probabilities, we calculate least squares estimates $(\bar{o}, \bar{w})$ for offset and base width for each template. To make the computation of the integrals efficient, we use the method proposed by Gallo et al., which is based on precalculating cells in $(o, w)$-space in which the distance between template and scanline is constant.

From the least squares estimates, the overlap between two templates at two consecutive positions can be calculated. Since the digits in the barcode don't overlap, the sequence of templates corresponding to the true patterns in the barcode should have small overlap in addition to the high individual matching probability. We use the dynamic programming scheme proposed in [3] to determine the sequence of templates which optimizes the matching and overlapping cost globally.

Finally, we calculate the first digit from the first six digit types (A or B). If the digit types don't form a valid pattern as described in the standard, we return a reading failure. If the check digit doesn't match, we return a failure as well.

Our implementation differs from the one described in [3] in the following ways:

- We extended the method from UPC barcodes to EAN-13 barcodes.

- Because there are no time constraints, we use a larger uncertainty $\Delta w$.

- If a digit lies next to a guard pattern, we extend the template by the guard pattern's bars.

Since we try a large number of scanlines, the same barcode might be read multiple times, or different scanlines might yield different barcode readings. We choose the returned barcode reading by the minimal total matching cost as well as favoring barcodes which have been read more often.
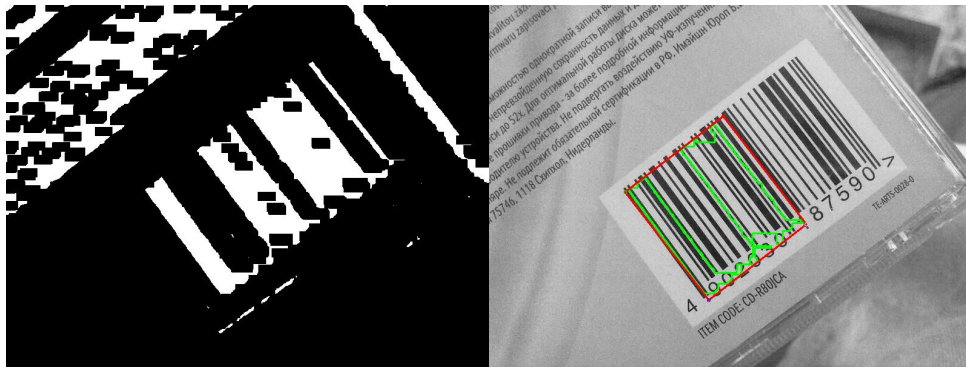
Figure 2: If the kernel size does not match to the barcode size Gradient+Blur fails to fully close the contour. The detected barcode is shown in red.

# 5 Comparison

## 5.1 Pros and Cons

**Gradient + Blur**

Pros:

Gradien+Blur is conceptually extremely simple and therefore extremely fast. It also is robust against disturbances like reflections since it only looks for the biggest contour.

Cons:

Since the algorithm uses the absolute gradient difference it is quite weak against rotations of 45 degrees. Gradient+Blur is also dependent on many parameters. If these parameters don't match up with the barcode the algorithm fails. One such instance is a too small kernel size for the closing step, which leads to a fragmented contour because it fails to close the white segments. An example of this can be seen in fig. 2. Another problem is the susceptibility to noise. Gradient+Blur could mistake the wrong contour for the barcode.

**LSD**

Pros:

The LSD is still relatively fast and can reliably detect a barcode in almost every position and rotation.

Cons:

The LSD looks for all parallel lines. If there are textures in the image with a large number of parallel lines, these could be mistaken for a barcode. Disturbances like reflections can also break barcode lines and lead to exclusion valid lines.

**Variation**

Pros:

The variation boundary finder is not dependent on the line segments returned by LSD, so that good boundaries can still be found even if the LSD result is bad due to glare spots, bad focus, etc.

Cons:

Structures with large variation next to the barcode, such as text, can result in the boundaries being extended beyond the barcode. Additionally, the bars of the outer guard patterns are very thin and may not result in enough variation, especially if there is some amount of blur. The variation boundary finder will tend to cut off the last few bars on each side.

**LSD Bound**

Pros:

Because of the high quality of line segments returned by LSD, this method is very good at accurately determining the boundary segments. We return multiple candidates on each side, so that some variance can be dealt with.

Cons:

Since it is strongly dependent on the LSD localization it fails as soon as the LSD localization fails. And since an enormous amount of lines needs to be tested the algorithms is not suited for real time applications.

**Wachenfeld**

Pros:

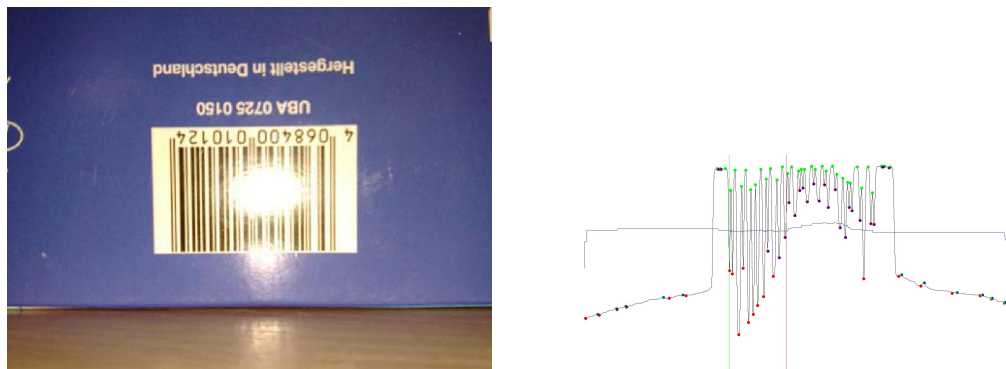The Wachenfeld algorithm is relatively quick since it is based on a scanline.

Figure 3: Preprocessin failing to apply dynamic thresholding and determining local extrema because of light reflections.

Cons:

The algorithm is strongly dependent on the quality of the preprocessing and detection of local extrema. And since the algorithm is based on a scanline it has no way to deal with broken barcodes caused by disturbances as seen in fig. 3. Finally, if the last segment selection steps misses, the barcode can be shifted to the left or right and become unreadable.

**Template Matching**

Pros:

Since no binarization is required, template matching is extremely robust against blurred barcodes. Some uncertainty in the localization and boundary detection can be dealt with.

Cons:

The matching process required precomputed data to be matched against the barcode. This can take a lot of time and memory depending on the targeted accuracy. And since the template matching is based on probability it is more likely to return a false positive result than no result.

## 5.2 Datasets

The implemented algorithms were tested on three datasets.

- Generated Barcodes:

- – 110 images, 300×150 px, barcode only.

- – 110 images, 1000×1000 px, barcodes (300×150 px) randomly rotated and translated on white background.

- WWU Muenster Barcode Database [7] [6]:
1055 images, 800×600 px.

- ArteLab Dataset - Robust Angle Invariant 1D Barcode Detection [8] [10] [9]:
2 sets of 215 images, 800×600 px.

## 5.3   Run time and Accuracy Comparison

The algorithms were compared over the 1055 images of the WWU Muenster Barcode Database [7]. The programm was implemented in C++ with the help of the Qt 5.7 and OpenCV 3.1 frameworks. The test were made on a Debian 8 system with an Intel N2940 CPU, 4 Cores / 4 Threads, and 4 GB RAM. The results are shown in fig. 4.

The experimental results illustrate the pros and cons of the various algorithms shown in section 5.1. The Gradient+Blur algorithm performs the best in respect to speed but the worst in respect to accuracy. The simplicity of the method is directly apparent, but the listed problems cause it to miss the boundaries or even fail to detect the barcode.

The second fastest algorithm is the Wachenfeld boundary detection. This is primary achieved through the usage of a single scanline. But the unoptimized preprocessing causes the algorithm to miss the boundaries in over 40% of tests since the dynamic thresholding fails to accurately binarize the scanline.

Both Variation Boundary Detection and LSDBounds take a very long time. This is caused by the multiple computation heavy probings of possible boundaries, which results in 126 different scanlines being read for each barcode. However, this allows a correct barcode to be read even if some boundary detections are invalid, which results in a high accuracy.

|                   | Errors | Accuracy | Time in sec. |
|-------------------|--------|----------|--------------|
| **Gradient + Blur** | 831    | 22%      | 266          |
| **LSD + Variation** | 279    | 74%      | 1595         |
| **LSD + LSDBounds** | 41     | 97%      | 1760         |
| **LSD + Wachenfeld** | 452   | 56%      | 319          |

Figure 4: Comparison of different algorithms on the WWU Muenster Barcode Database. All algorithms use Template Matching to read the barcode.

# 6  Improvements

In this section, we will consider some possible improvements to our implementation of the algorithms.

## 6.1  Gradient+Blur Detection

### Vary by rotation

Since the Gradient+Blur-detection builds from the absolute gradients found by the Sobel operator, results might be poor when a barcode is rotated close to 45 degrees. To remedy this, we might run the detection on rotated versions of the image. Rotating once by 45 degrees would yield the greatest improvement, however, multiple rotations could be checked at diminishing returns.

### Vary kernel sizes

In our current implementation, all operations (blurring, closing, opening) are applied with a constant kernel size. This is somewhat problematic, since the effectiveness of these parameters is dependent on the size of the barcode. If a barcode is not detected successfully, we might try different kernel sizes.
The initial kernel size might also be considered further: The current values have been empirically determined to be most useful for the image sizes we worked with. Scaling the kernel size appropriately for each image might lead to better results, since it seems likely that the relative sizes barcodes in images is independent of image resolution.

## 6.2   LSD

**Unite interrupted line segments**

A remaining common failure of the LSD algorithm is it's poor handling of reflections on the barcode. These reflections visually interrupt the barcode lines, so two short line segments are returned instead of one. This is problematic, as length of line segments is an important factor in deciding whether two line segments might be part of the same barcode. This ultimately leads to a split in the barcode, where the detected area covers just the larger side of the code.

This problem could be fixed in two related ways: First, we could try a *line segment unification*. This process would seek to unite line segments which lie on the same line in space. This easy calculation would unite line segments across gaps, thus restoring the proper length and avoiding rejection. To avoid uniting many stray lines across the image, simply limit unification to line segments where the gap size is less than some small multiple of the segment size itself.

This first approach has the weakness of only working when the reflection splits the line segment into two parts. Even better would be an approach that could handle a missing endpoint. This should be handled by this second approach, which is also more complicated: Instead of uniting line segments, we would now consider the endpoints of line segments in a second pass over all segments. During the first pass, whenever a pair of lines is considered to likely be part of the same barcode, save the location of their endpoints in two different lists, based on distance from the origin. After this first pass, those lists can easily construct the upper and lower bound of the barcode. With this new information, discard the previous scores and redo them. However, this time, instead of checking for similar length, check whether two line segments have an endpoint near one of those two lines before assigning a score to them. This second pass will now also handle missing endpoints.

## 6.3   Wachenfeld

**Better pruning, multiple scanlines**

The pruning of unusually high minima / low maxima is a very sensitive part of the algorithm, but is not described in detail in the paper. Further tuning of this step could possibly improve the performance. Also, we could detect along multiple scanlines and vote for most likely boundaries.

## 6.4   Template Matching

**Precompute patterns for blur of various strengths**

While the algorithm is already very capable in handling blurred barcodes, this might be improved even further by precomputing patterns specifically not for an ideal, clean barcode, but for one that is already blurred. False positives could be eliminated by returning a reading failure if the total matching cost is above a certain threshold.

# 7  Conclusion

In this work we have seen how different algorithms compare against each other in detecting barcodes.

After some initial comparisons of Gradient+Blur and LSD we decided to go with the latter because of the superior localization quality. And since we were satisfied with the high quality of the readings performed by the Template Matching we decided to focus our efforts on improving the overall accuracy by implementing additional boundary detection algorithms.

While comparing the Wachenfeld boundary detection against the Variation boundary detection we have shown that by sacrificing speed and increasing complexity we can increase the detection rate. Since we wanted to maximize the overall accuracy with regards to the competition within the scope of the project we improved on the Variation boundary detector by sacrificing more time and resources in favor of the LSDBound algorithm.

Obviously our methodology is not applicable for real time usage in the wild. A more fitting approach would be to implement a fast and simple algorithm like gradient blur enhanced with additional scan line based refinement like the Wachenfeld algorithm with optimized preprocessing and reading step. In a real time application the algorithm could depend on the user to provide sharp and disturbance free images with centered barcodes without rotation.

Finally our work can be summarized with: Higher accuracy detection and recognition of barcodes in a non-constrained system takes more time and resources.

# References

[1] G. Bradski. *cv::LineSegmentDetector Class Reference*. Mar. 20, 2017. URL: `http://docs.opencv.org/3.1.0/db/d73/classcv_1_1LineSegmentDetector.html`.

[2] Clement Creusot and Asim Munawar. "Low-computation egocentric barcode detector for the blind". In: *Image Processing (ICIP), 2016 IEEE International Conference on*. IEEE. 2016, pp. 2856–2860.

[3] Orazio Gallo and Roberto Manduchi. "Reading 1D barcodes with mobile phones using deformable templates". In: *IEEE transactions on pattern analysis and machine intelligence* 33.9 (2011), pp. 1834–1843.

[4] Rafael Grompone von Gioi et al. "LSD: a Line Segment Detector". In: *Image Processing On Line* 2 (Mar. 2012), pp. 35–55. DOI: `10.5201/ipol.2012.gjmr-lsd`.

[5] GS1. *GS1 General Specifications*. Jan. 2017. URL: `http://www.gs1.org/barcodes-epcrfid-id-keys/gs1-general-specifications`.

[6] Steffen Wachenfeld, Sebastian Terlunen, and Xiaoyi Jiang. "Robust recognition of 1-d barcodes using camera phones". In: *Pattern Recognition, 2008. ICPR 2008. 19th International Conference on*. IEEE. 2008, pp. 1–4.

[7] Steffen Wachenfeld, Sebastian Terlunen, and Xiaoyi Jiang. *WWU Muenster Barcode Database*. URL: `http://cvpr.uni-muenster.de/research/barcode`.

[8] Alessandro Zamberletti, Ignazio Gallo, and Simone Albertini. *Robust Angle Invariant 1D Barcode Detection*. Proceedings of the 2nd Asian Conference on Pattern Recognition (ACPR), Okinawa, Japan. 2013. URL: `http://artelab.dista.uninsubria.it/downloads/datasets/barcode/hough_barcode_1d/hough_barcode_1d.html`.

[9] Alessandro Zamberletti, Ignazio Gallo, and Simone Albertini. "Robust angle invariant 1d barcode detection". In: *Pattern Recognition (ACPR), 2013 2nd IAPR Asian Conference on*. IEEE. 2013, pp. 160–164.

[10] Alessandro Zamberletti et al. "Neural Image Restoration for Decoding 1-D Barcodes using Common Camera Phones." In: *VISAPP (1)*. 2010, pp. 5–11.